LAWRENCE
LIVERMORE
NATIONAL
LABORATORY

LX-17 and ufTATB Data for Corner-Turning, Failure and Detonation

P. C. Souers, L. Lauderbach, R. Garza, P. Vitello, D. E. Hare

February 16, 2010

Disclaimer

This document was prepared as an account of work sponsored by an agency of the United States government. Neither the United States government nor Lawrence Livermore National Security, LLC, nor any of their employees makes any warranty, expressed or implied, or assumes any legal liability or responsibility for the accuracy, completeness, or usefulness of any information, apparatus, product, or process disclosed, or represents that its use would not infringe privately owned rights. Reference herein to any specific commercial product, process, or service by trade name, trademark, manufacturer, or otherwise does not necessarily constitute or imply its endorsement, recommendation, or favoring by the United States government or Lawrence Livermore National Security, LLC. The views and opinions of authors expressed herein do not necessarily state or reflect those of the United States government or Lawrence Livermore National Security, LLC, and shall not be used for advertising or product endorsement purposes.

LX-17 and ufTATB Data for Corner-Turning, Failure and Detonation

P. Clark Souers, Lisa Lauderbach, Raul Garza, Peter Vitello and David E. Hare
Energetic Materials Center L-282
Lawrence Livermore National Laboratory, Livermore, CA USA 94550

Abstract. Data is presented for the size (diameter) effect for ambient and cold confined LX-17, unconfined ambient LX-17, and confined ambient ultrafine TATB. Ambient, cold and hot double cylinder corner-turning data for LX-17, PBX 9502 and ufTATB is presented. Transverse air gap crossing in ambient LX-17 is studied with time delays given for detonations that cross.

_____

Experimental Methods

We have worked several years on multiple LX-17 (92.5% TATB, 7.5% Kel-F 800) measurements as input to advanced kinetic models that can handle detonation, corner-turning with dead zone formation and detonation failure [1-3]. We here add to this data.

Perhaps the most basic is the size (diameter) effect, where the detonation velocity is plotted as a function of the inverse explosive radius of a cylinder [4]. The cylinder may be confined, which means copper here, or unconfined, which means mostly Lucite but sometimes bare on a rack. The explosive is ram-pressed, usually into 25.4 mm-long pellets, which are placed end-to-end in a vertical tube. The ambient gap is between the pellet edge and the inside wall is about 0.025 mm. When cooled to -55°C, which is "cold" in this paper, a TATB explosive linearly contracts by 0.38% but the copper moves only 0.12%. The difference of 0.24% amounts to 0.03 mm for a 12.7-mm radius cylinder. This volume is filled with bubble-eating grease. The chilling is obtained by passing liquid-nitrogen-cooled gas through a plastic chamber containing the cylinder.

The densities in this paper are LX-17 1.90 g/cm^3, PBX 9502 1.89 g/cm^3 and ultrafine TATB (ufTATB) 1.80 g/cm^3, all to $\pm$0.01 g/cm^3. The ufTATB is measured is measured like a main charge because it is the booster for the others, but we are using main charge code models on it for the first time. In driving LX-17 and PBX 9502, a 25.4 mm-long booster of 1.71 g/cm^3 Comp B is used.

The measurements are made with shorting pins with the intention of finding the steady state detonation velocity. The length of the tube is set to over 11 radii long or more. The usual procedure is to place two rings with 6 pins each near the end farther from the detonator. The position and pulse arrival time for each pin is plotted and the outlier data is not used. The resulting standard deviation of the pin velocities is the precision.

Some of the data is taken with embedded fiber optic (EFO) [5]. This requires drilling a 1.60 mm diameter hole on-axis through the explosive. A probe of aqueous cesium chloride in a polytetrafluroethylene pipe runs down the length of the hole. Fabry-Perot interferometry [6-8] looks down the probe cable and is reflected back from the shock front formed as the explosive crushes inward into the fiber. Figure 1 shows the shot #225 EFO detonation velocity of a 12.7 mm-radius 1.91 g/cm^3 LX-17 cylinder in Lucite being driven by a 1.83 g/cm^3 PBX 9501 booster [9]. The distance along the axis is plotted in units of the radius, L/R$_o$. It appears that the velocity levels off after 6 radii at 7.535 mm/µs, which is close to the value obtained in the size effect shots, so it appears that we are indeed at steady state.
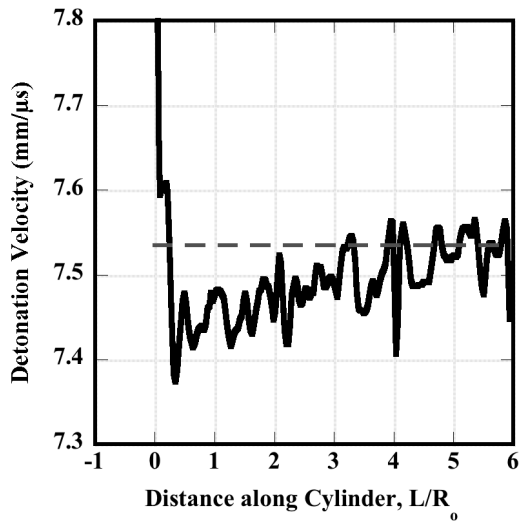
Fig. 1. Fiber-measured detonation velocity of LX-17 being boosted by PBX 9501.

We are also interested in the time delay for the detonation front caused by the gaps. The no-gap ratestick does not go all the way to steady state, but we can estimate a fit of

$$U_s \approx 7.42 + 0.12\,exp(-0.025L), \qquad (1)$$

where U_s is the detonation velocity and L is the distance from the end of the booster pellet, obtained by integration of the time data. We then have the relation

$$t = \left(5.437e-4\right) + 0.1345L - \left(1.265e-5\right)L^2, (2)$$

which can be extrapolated to the estimated steady state value. We now subtract the fiducial

The transverse gap measurements all use ambient LX-17 as an acceptor with an air gap between that and some donor explosive, which is usually LX-17 of some number of pellets. Most of the explosives lie bare on a rack but the 25.4 mm–radius shots are confined in copper with 3.1-3.8 mm wall thicknesses. An RP-1 is used to detonate the donor, but the donor length is usually short enough that the detonation is not at steady state once it reaches the gap. The acceptor set uses four to six 25.4 mm-long LX-17 pellets, so that the 100-150 mm run probably shows whether the detonation re-ignites or not. Pins are placed all along the array, with two set close to the gap on either side. An approximate detonation velocity on either side is needed to

time measured with the gap and convert to time units with the gap edge reset as zero.

The double cylinder is used for corner-turning, and the schematic is shown in Figure 2. An RP-1 detonator detonates a 63.5 mm-long, 6.35 mm-radius small cylinder of 1.77-1.78 g/cm^3 LX-14, which is actually made of five pellets. The main charge is 25.4 mm radius and 25.4 or 50.8 mm long, made of two ram-pressed pieces. A washer is placed at the intersection of the two cylinders. It is usually steel of 6.35 mm thickness but some 3.18 and 63.5 mm plastic washers were also used. The breakout times are measured by a line of shorting pins along the outer surface of the large cylinder, and they are referenced to the intersection of the large cylinder and the washer. Time zero is the point between the LX-14 and the large cylinder. One or two pins are placed on the LX-14 and this allows an interpolation as to zero time. Many times, there is also a pin at the far end of the large cylinder. If the dead zone is large, as with LX-17, this can disrupt the measurement down the axis to the far pin.
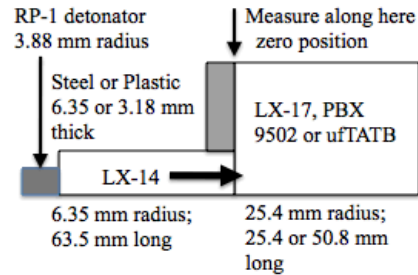

Fig. 2. Schematic of the double cylinder. The bottom line is an axis of revolution.

extrapolate to the zero time at the start of the gap.

Experimental Results

The size effect results are listed in Table 1 for LX-17 confined in copper at ambient and -55°C. Included also is unconfined LX-17 taken mostly in Lucite. Bare samples on a rack mount are listed as "P" for pins and "E" for EFO-measured. Some of the results are shown in Figure 3. The data here for confined and unconfined LX-17 is about the same whereas the ufTATB clearly has a shallower slope. If we use

the estimation equation for an average detonation rate, ν (in μs^{-1})[10]

$$\nu = \frac{-D^2}{\partial U_s / \partial(1/R_o)}, \qquad (3)$$

we get a rate of 37-45 μs^{-1} for LX-17 and 100-110 μs^{-1} for ufTATB. We believe that the minimum zoning in modeling in zone/cm is about the same as the rate, so that the booster here requires more than twice the zoning of the LX-17.
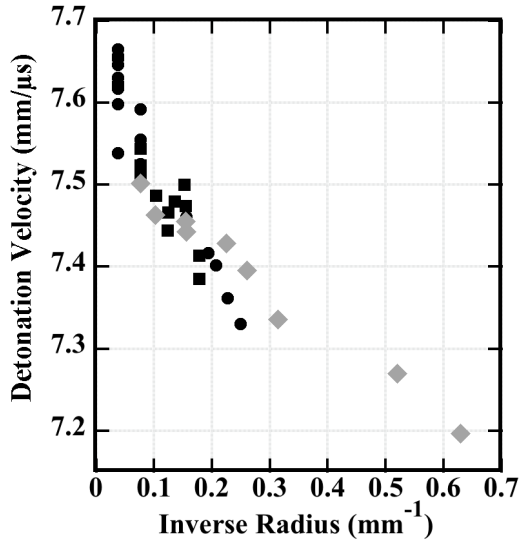

Fig. 3. Size effect curves for ambient confined (circles) and unconfined (squares) LX-17 and ufTATB (gray diamonds).

The points listed in Table 1 as "failure" showed no pin signals. However, a few returned low velocities such as the 6.89 mm/μs value seen with ambient confined LX-17. This is a real but probably failing signal, and it is reminiscent of the low values seen in PBX 9404 and PBX 9501 at small sizes [11]. This suggests that failure is not a sharp phenomenon but shows variability over a size range.

The corner-turning results are listed in Table 2. Some of the average steel-backed data is shown in Figure 4. The Huygens line from the top of the LX-14 directly to the edge of the larger cylinder is given by the ambient ufTATB and the latter part of the ambient LX-17 curve.

All displacements above this line indicate a delay. That this delay is caused by a dead zone with no probable chemical reaction has been seen by X-rays and proton radiography [1, 12-17]. Heat clearly reduces the dead zone and cold makes it larger.

Some of the last entries with shorter times are the end-of-the-pellet, on-axis times.
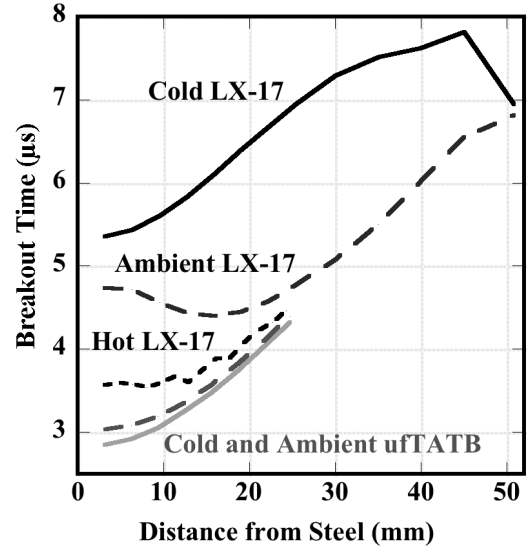

Fig. 4. Average breakout times for steel-backed double cylinders.

The transverse air gap data taken since reference 3 is listed in Table 3. The times are zeroed at the start of the gap. The standard of "no gap" is the EFO shot shown in Figure 1. Using this, we can calculate the time delays seen at each pin on the acceptor side. If the delays jump to high values with pin signals then failing, then the acceptor did not re-detonate. For donor pellets of LX-17 of a given length L (in mm), we distill the data to this 50% probability of detonation gap width Δx (in mm)

$$\Delta x(50\%) \approx \left[L(donor) \right]^{0.27}. \qquad (4)$$

This covers three donor lengths at 25.4, 50.8 and 152.4 mm, with the last being steady state.

The measured time delays are shown in Figure 5. All pin-measured samples were fired with 1.71 g/cm^3 Comp B boosters. One was an EFO point done with the PBX 9501 booster [9]. Two EFO shots were done for this report using Comp B boosters. The difference in boosters

made no difference, even though the points were transient. Previously, we thought these results might be a function of the detonation front curvature, but the current data shows a division between transient and steady state data, with the latter showing longer delays. The upper steady state and the lower transient curves may be fit by

$$\Delta t(\,steady-state\,) \approx 0.76(\Delta x)^{0.62}$$
$$\dot{\Delta}t(\,transient\,) \approx 0.32(\Delta x)^{0.69} \quad (5)$$

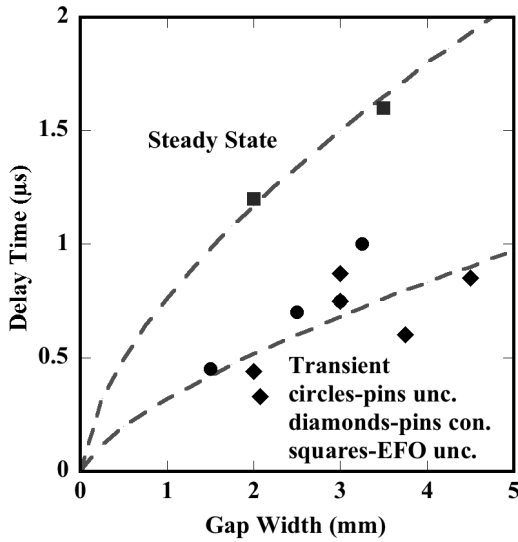with the time delay Δt in µs and the gap Δx in mm.

Fig. 5 Time delays in LX-17 caused by transverse air gaps.

It must be admitted that these time delays are approximate and are a function of time themselves. Figure 6 shows five measured curves by three techniques. There appears to be little difference between the outside edge results from the pins and the on-axis EFO except for an initial spike with the pins. All curves tend upwards and it appears that the 152 mm of acceptor used in the steady state runs was not long enough.

SUMMARY

The quest is on to find a model that describes all these features simultaneously. In calibrating our Tarantula model for ambient LX-17[3], we first set the detonation velocity of the 5

mm-radius cylinder at 7.39-7.41 mm/µs. Then, we run the 12.7 mm-radius cylinder for a detonation velocity of 7.54-7.56 mm/µs. If a JWL is used, the Cylinder wall velocities will automatically agree, it we run CHEETAH, a thermochemical model [18], then we need to adjust for the measured velocities as well. Next, we run the double cylinder, where the rate constant of the LX-14 becomes a knob. This is because we can get the necessary zoning for the LX-17 but not the ideal booster, so that any description of it
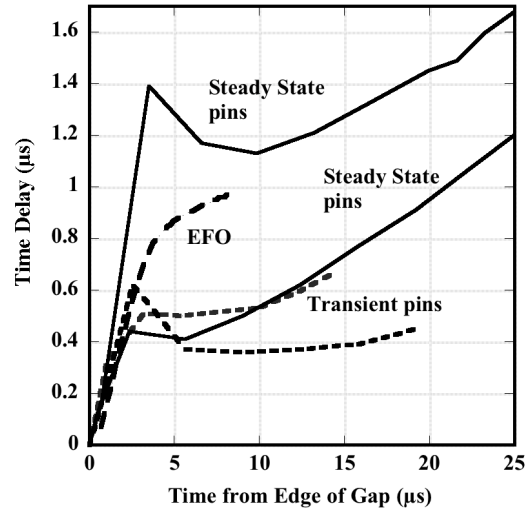
Fig. 6. Time dependence of the time delays.

will be wrong. Finally, we run the 3 mm-radius cylinder for failure. The separation of the 5 mm cylinder as the smallest detonating size and 3 mm is set so as to be fairly sure of the result in both cases. The gap crossing data does not constitute a primary model test at this time. Tarantula does the go-no go part fairly well but only gets about half of the time delay.

Getting all this to work in Tarantula is difficult, and the results vary with zoning and artificial viscosity. In many cases, setting the 3 mm failure properly creates dead zones that are too big and fixing the dead zones makes the 3 mm size detonate. If we run unconfined LX-17 at 7 mm-radius (7.39-7.41 mm/µs) and 4.5 mm for failure, we find the entire package is easier to get. The EFO failure results reported at this conference by T. Lorenz [19] are measured bare

and so are easier to model, although the 5.08 mm-radius sample may or may not fail. The conclusion is that one Tarantula setting does not do dead zones and confined failure. Another aspect comes with the Jackrabbit series done by M. Hart [20]. His metal plates have explosive behind them and the only way to model the back edge movement is to add a desensitization package. Little data exists on desensitization, so the model becomes more ambiguous.

Table 1. Summary of LX-17 and ufTATB steady state size effect data.

Radius (mm)	Detvel (mm/μs)	stdev (mm/μs)	Wall (mm)	Length (mm)	Radius (mm)	Detvel (mm/μs)	stdev (mm/μs)	Wall (mm)	Length (mm)
LX-17, Ambient-Confined in Copper					6.40	7.473	0.051	1.50	152
25.42	7.629		5.19	300	6.35E	7.37	rising		51
25.42	7.537		5.18	300	6.35E	7.38	rising		51
25.42	7.616		2.72	300	5.56	7.384	0.017	1.59	152
25.42	7.656		2.72	300	5.55P	7.412	0.056		254
25.42	7.652		2.72	300	5.55P	failed			254
25.41	7.597		5.21	300	5.10	7.140	0.069	1.22	152
25.41	7.621		2.72	300	5.08E	failed			51
25.41	7.645		2.71	300	5.08E	failed			51
25.41	7.664		2.71	300	5.06P	failed			255
25.41	7.623		2.72	300	3.83	failed		0.96	153
12.71	7.554	0.016	2.60	305	3.81E	failed			51
12.71	7.591		1.37	300	3.81E	failed			51
12.66	7.524	0.010	3.16	1067	LX-17, cold-Confined in copper				
6.37	7.459	0.019	1.34	152	25.62	7.570	0.006	5.03	458
5.11	7.415	0.046	2.82	156	12.76	7.465	0.017	2.55	305
4.78	7.400	0.024	3.18	254	9.51	7.476	0.071	3.20	155
4.38	7.360	0.040	1.97	156	8.04	7.445	0.150	3.00	152
3.98	7.329	0.017	2.37	255	6.37	7.444	0.038	1.35	153
3.83	failed		2.52	153	6.34	7.36	0.054	1.60	155
3.81	failed		2.46	154	5.60	fail		1.54	254
3.18	6.891	0.10	3.18	152	5.58	7.354	0.074	2.35	154
3.20	failed		3.15	459	4.79	fail		0.94	252
3.20	failed		3.15	280	4.47	fail		1.93	252
LX-17, Ambient-Unconfined (Lucite or bare)					TATB, ambient in copper				
12.73	7.543	0.027	3.16	102	12.71	7.500	0.035	2.60	305
12.70	7.522	0.013	3.25	330	9.59	7.462	0.024	3.17	152
12.70	7.509	0.015	3.25	330	6.41	7.454	0.050	1.42	152
9.53	7.485	0.009	1.66	254	6.37	7.441	0.017	1.35	152
7.97	7.443	0.038	1.56	253	4.41	7.427	0.041	1.51	153
7.95	7.465	0.026	1.61	203	3.81	7.394	0.034	2.24	154
7.29P	7.478	0.046		305	3.16	7.334	0.045	3.16	153
6.49	7.499	0.030	1.45	249	1.91	7.268	0.058	2.86	154
					1.59	7.195	0.015	1.60	156

Table 2. Double cylinder data, showing the breakout times along the circular edge parallel to the detonation.

distance (mm)	time (μs)	distance (mm)	time (μs)	distance (mm)	time (μs)	distance (mm)	time (μs)
LX-17 cold #6-1		22.23	6.98	25.88	3.44	#9-5, steel	
steel		25.40	7.28	PBX 9502 ambient		3.15	3.45
3.18	5.40	30.00	7.69	#9-1, steel		4.78	3.36
6.35	5.49	35.00	8.08	3.18	4.15	6.40	3.31
9.53	5.69	40.00	8.37	6.30	3.99	8.03	3.39
12.70	5.94	45.00	8.56	9.43	3.93	9.65	3.37
15.88	6.24	50.80	6.82	12.56	3.93	11.28	3.41
19.05	6.55	LX-17, cold, #6-4		15.69	4.02	12.90	3.53
22.23	6.87	thin plastic		18.82	4.17	14.53	3.59
25.40	7.17	3.18	5.61	21.95	4.38	16.15	3.65
30.00	7.58	6.35	5.69	25.08	4.63	17.78	3.78
35.00	7.92	9.53	5.81	25.88	3.43	19.41	3.91
40.00	8.17	12.70	6.01	PBX 9502 cold		21.03	4.00
45.00	8.34	15.88	6.22	#10-1, steel		22.66	4.16
50.80	6.88	19.05	6.44	3.11	5.15	24.28	4.33
LX-17, cold, #6-3		22.23	6.64	7.35	5.27	25.89	3.30
steel		25.40	6.83	11.57	5.63	ufTATB ambient	
3.18	5.31	30.00	7.05	17.92	5.85	#9-2, steel	
6.35	5.38	35.00	7.19	22.16	6.16	3.18	2.85
9.53	5.52	40.00	7.23	24.27	5.69	6.26	2.92
12.70	5.73	45.00	7.37	28.96	5.93	9.34	3.05
15.88	5.97	50.80	6.83	31.06	5.68	12.42	3.25
19.05	6.22	LX-17 hot #9-6		33.20	5.91	15.50	3.47
22.23	6.47	steel		37.41	6.09	18.58	3.73
25.40	6.71	3.16	3.57	41.66	6.67	21.66	4.03
30.00	6.98	4.79	3.59	48.01	7.28	24.74	4.32
35.00	7.11	6.41	3.58	PBX 9502 cold		25.55	3.42
40.00	7.07	8.04	3.54	#9-4, steel		ufTATB cold	
45.00	7.29	9.66	3.59	3.18	5.12	#9-3, steel	
50.80	7.00	11.29	3.67	6.29	5.27	3.20	3.04
LX-17 cold #6-2		12.92	3.60	9.40	5.47	6.27	3.08
plastic		14.54	3.76	12.51	5.68	9.35	3.19
3.18	5.33	16.17	3.89	15.62	5.85	12.42	3.35
6.35	5.57	17.79	3.90	18.73	5.76	15.49	3.56
9.53	5.81	19.42	4.08	21.84	5.60	18.57	3.82
12.70	6.07	21.04	4.22	24.96	5.64	21.64	4.10
15.88	6.36	22.67	4.32	25.51	3.46	24.71	4.39
19.05	6.67	24.30	4.46	PBX 9502 hot		25.54	3.41

Table 3. Transverse air gap crossing data into LX-17 as measured by pins.

Pellets/ Gap	Position (mm)	Time (µs)	Delay (µs)	Gap (mm)	Position (mm)	Time (µs)	Delay (µs)
2 LX-17	-38.26	-5.06			121.48	16.31	0.62
crossed	-12.75	-1.69			138.44	18.56	0.72
2.5 mm	-0.80	-0.11			153.84	20.57	0.77
	0.00	0.00	0.00	2 LX-17	-84.73	-11.02	
	3.29	0.49	0.06	copper-	-67.79	-8.85	
	15.31	3.05	1.02	confined	-33.91	-4.42	
	40.95	6.04	0.63	50.8 mm	-16.95	-2.24	
	66.51	9.42	0.65	crossed	-1.59	-0.21	
	92.00	12.78	0.69	3.75 mm	0.00	0.00	0.00
	103.95	14.36	0.71		5.34	1.01	0.32
2 LX-17	-38.23	-5.03			20.97	3.24	0.51
crossed	-12.75	-1.67			38.19	5.47	0.50
3. 0 mm	-0.80	-0.11			72.30	9.91	0.53
	0.00	0.00	0.00		89.21	12.14	0.59
	3.80	0.62	0.12		104.52	14.18	0.66
	15.73	3.30	1.21	2 LX-17	-84.83	-11.00	
	41.20	6.26	0.79	copper-	-67.86	-8.86	
	66.69	9.58	0.76	confined	-33.93	-4.45	
	92.17	12.96	0.79	50.8 mm	-16.97	-2.23	
	104.92	14.53	0.70	crossed	-1.59	-0.21	
2 LX-17	-38.21	-5.04		4.5 mm	0.00	0.00	0.00
failed	-12.74	-1.68			6.09	1.21	0.41
4.0 mm	-0.80	-0.11			21.46	3.58	0.78
	0.00	0.00	0.00		38.45	5.73	0.72
	4.80	0.67	0.04		72.41	10.15	0.76
	16.74	3.54	1.32		89.40	12.37	0.79
	42.22	7.27	1.67		104.80	14.41	0.85
	67.71	13.77	4.81	1 of	-12.68	-1.52	
3 LX-17	-63.96	-8.47		ufTATB	-0.79	-0.11	
crossed	-38.42	-5.10		failed	0.00	0.00	
3.25 mm	-12.84	-1.68		1.5 mm	2.30	0.31	
	-1.59	-0.21			14.21	2.99	
	0.00	0.00	0.00		39.81	10.79	
	4.84	0.92	0.28	2.5	-12.69	-1.55	
	16.02	3.88	1.77		-0.79	-0.11	
	41.55	6.31	0.85		0.00	0.00	
	67.06	9.66	0.87		3.29	0.46	
	92.55	13.00	0.90		15.21	3.31	
	103.71	14.49	0.94		40.65	11.12	
	103.72	14.62	1.07	1 TNT	-7.20	-0.93	
2 LX-17	-84.31	-10.97		6x6 mm	-1.59	-0.22	
copper-	-67.52	-8.81		failed	0.00	0.00	
confined	-33.82	-4.41		1.25 mm	2.84	0.24	
50.8 mm	-16.90	-2.22			9.23	1.70	
crossed	-1.59	-0.21			21.20	5.48	
3.0 mm	0.00	0.00	0.00	1 LX-14	-6.35	-0.85	
	4.59	0.88	0.28	6x6 mm	-0.79	-0.11	
	19.93	3.03	0.43	failed	0.00	0.00	
	36.84	5.24	0.44	1.25 mm	2.04	0.33	
	73.68	9.67	0.12		7.60	1.53	
	87.59	11.88	0.54		20.33	5.34	

References

1. Souers, P. C., Andreski, H. G., Cook III, C. F., Garza, R., Pastrone, R., Phillips, D., Roeske, F., Vitello, P. and Molitoris, J. D.,"LX-17 Corner Turning," *Propellants, Explosives, Pyrotechnics*, 29 [6], 359, 2004.

2. Souers, P. C., Andreski, H. G., Batteux, J., Bratton, B., Cabacungan, C., Cook III, C. F., Fletcher, S., Garza, R., Grimsley, D., Handly, J., Hernandez, A., McMaster, P., Molitoris, J. D., Palmer, R., Prindiville, J., Rodriguez, J., Schneberk, D., Wong, B. and Vitello, P., "Dead Zones in LX-17 and PBX 9502, *Propellants, Explosives, Pyrotechnics*," 31 [2], 89-97, 2006.

3. Souers, P. C., Hernandez, A., Cabacungan, C., Fried, L., Garza, R., Glaesemann, K., Lauderbach, L., Liao. S.-B., and Vitello, P., "Air Gaps, Size Effect, and Corner-Turning in Ambient LX-17," *Propellants, Explosives, Pyrotechnics*, 34 [1], 32-40, 2009.

4. Eyring, H., Powell, R. E., Duffey, G. H., and Parlin, R. B., "The Stability of Detonation," *Chem. Rev. 45*, 69-179, 1949.

5. Hare, D. E., Goosman, D. R., Lorenz, K. T., and Lee, E. L., "Application of the Embedded Fiber Probe in High Explosive Detonation Studies: PBX 9502 and LX-17," *Thirteenth International Detonation Symposium*, Norfolk, VA, July 23-28, 2006, 1081-1091.

6. Goosman, D. R., Wade, J. T., Garza, R. G., Avara, G. R., Crabtree, T. R., Rivera, A. T., Hare, D. E., Tolar Jr., D. R., and Bratton, B. A., "Optical Probes for Continuous Fabry-Perot Velocimetry inside Materials," 26th International Congress on High-Speed Photography and Photonics, D. L. Paisley, ed, *Proceedings of the SPIE*, 5580, 517-528, 2005.

7. Goosman, D., Avara, G., Steinmetz, L., Lai, C., and Perry, S., "Manybeam Velocimeter for Fast Surfaces," Lawrence Livermore National Laboratory report UCRL-JC-123809, 1996.

8. Goosman, D., Avara, G., Wade, J., and Rivera, A., "Optical Filters to exclude Non-Doppler-Shifted Light in Fast Velocimetry," Lawrence Livermore National Laboratory report UCRL-JC-145646-REV-1, 2002.

9. Hare, D. E., Chandler, J. B., Compton, S. M., Garza, R. G., Grimsley, D. A., Hernandez, A., Villafana, R. J., Wade, J. T., Weber, S. R., Wong, B. M., and Souers, P. C., "Propagation or Failure of Detonation across an Air Gap in an LX-17 Column: Continuous Time-Dependent Detonation or Shock Speed using the Embedded Fiber Optic (EFO) Technique," Lawrence Livermore National Laboratory report LLNL-TR-400791, 2008.

10. Souers, P. C., Anderson, S., McGuire, E., Murphy, M. J., and Vitello, P., "Reactive Flow and the Size Effect," *Propellants, Explosives, Pyrotechnics*, 26, 26-32, 2001.

11. *LASL Explosive Property Data*, Gibbs, T. R., and Popolato, A., ed.. University of California Press, Berkeley, 1980, section following p. 236.

12. Venable, D., and Boyd, Jr., T. J., "Phermex Applications to Studies of Detonation Waves and Shock Waves," *Proceedings Fourth Symposium (International) on Detonation*, White Oak, MD, October 12-15, 1965, pp. 639-647.

13. Rivard, W. C., Venable, D., Fickett, W., and Davis, W. C., Flash X-Ray Observation of Marked Mass Points in Explosive Products, *Proceedings Fifth Symposium (International) on Detonation*, Pasadena, CA, August 18-21, 1970, pp. 3-11.

14. Mader, C. L., "Two Dimensional Homogenous and Heterogeneous Detonation Wave Propagation," *Proceedings Sixth Symposium (International) on Detonation,* Coronado, CA, August 24-27, 1976, pp. 405-413.

15. Zumbro, J. D., Adams, K. J., Alrick, K. R., Amann, J. F, Boissevain, J. G., Crow, M. L., Cushing, S. B., Clark, D., Eddleman, J. C., Espinoza, C. J., Ferm, E. N., Fife, T. T., Gallegos, R. A., Gomez, J., Gray, N. T., Hogan, G. E., Holmes, V. H., Jramillo, S. A., King, N. S.

P., Knudsen, J. N., London, R. K., Lopez, R. P., McClelland, J. B., Merrill, F. E., Morley, K. B., Morris, C. L., Pazuchanics, P. D., Pillai, C., Riedel, C. M., Sarracino, J. S., Saunders, A., Stacy, H. L., Takala, B. E., Trujillo, O., Tucker, H. E., Wilke, M. D., Yates, G. J., Ziock, H. J., Balzer, S., Flores, P. A., and R. T. Thompson, "Proton Radiography of the Detonation Front in HE Systems," *Eleventh International Detonation Symposium,* Snowmass Village, CO, August 31-September 4, 1998, pp. 54-65.

16. Mader, C. L., Zumbro, J. D., and Ferm, E. N., "Proton Radiographic and Numerical Modeling of Colliding, Diverging PBX 9502 Detonations," *12th International Detonation Symposium*, August 11-16, 2002, San Diego, CA, 55-60.

17. Ferm, E. N., Morris, C. L., Quintana, J. P., Pazuchanic, P., Stacy, H., Zumbro, J. D., Hogan, G., and King, N., "Proton Radiography Examination of Unburned Regions in PBX 9502 Corner Turning Experiments," 12th *American Physical Society Topical Conference on Shock Compression in Condensed Matter*, Atlanta, GA, June 24-29, 2001, pp. 966-969.

18. Vitello, P., Fried, L., Glaesemann, K., and Souers, C., "Kinetic Modeling of Slow Energy Release in Non-Ideal Carbon Rich Explosives," *Thirteenth International Detonation Symposium*, Norfolk, VA, July 23-28, 2006, pp. 465-475.

19. K.T. Lorenz, D. Hare, R. Chambers, P.Vitello, P.C. Souers and E.L. Lee, "Detonation Failure in Small Cylindrical LX-17 Charges," this conference.

20. Mark M. Hart, "Jack Rabbit Investigation Of TATB IHE Detonation Chemical Kinetics," this conference.